Journal of Colloid and Interface Science 658 (2024) 179–187

Contents lists available at ScienceDirect

Journal of Colloid And Interface Science

journal homepage: www.elsevier.com/locate/jcis

Liquid-liquid surfactant partitioning drives dewetting of oil from hydrophobic surfaces

Kueyoung E. Kim [a,1,2], Wangyang Xue [a,1,2], Lauren D. Zarzar [a,b,c,2,*]

[a] Department of Chemistry, The Pennsylvania State University, University Park, PA 16802, USA
[b] Department of Materials Science and Engineering, The Pennsylvania State University, University Park, PA 16802, USA
[c] Materials Research Institute, The Pennsylvania State University, University Park, PA 16802, USA

GRAPHICAL ABSTRACT

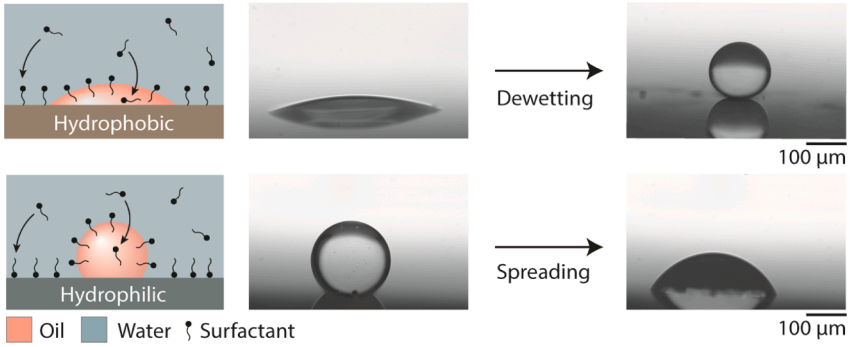

ARTICLE INFO

Keywords:
Wetting
Surfactant
Adsorption
Partitioning
Sessile Droplet

ABSTRACT

Hypothesis: Sessile droplets solubilizing in surfactant solution are frequently encountered in practice, but the factors governing their non-equilibrium dynamics are not well understood. Here, we investigate mechanisms by which solubilizing, sessile oil droplets in aqueous surfactant solution dewet from hydrophobic substrates and spread on hydrophilic substrates.

Experiments: We quantify the dependence of droplet contact line dynamics on drop size and oil, surfactant, and substrate chemistries. We consider halogenated alkane oils as well as aromatic oils and focus on common nonionic nonylphenol ethoxylate surfactants. We correlate these results with measurements of the interfacial tensions.

Findings: Counter-intuitively, under a range of conditions, we observe complete dewetting of oil from hydrophobic substrates but spreading on hydrophilic substrates. The timescales needed to reach a steady-state contact angle vary widely, with some droplets examined taking over a day. We find that surfactant surface adsorption governs the contact angle on shorter timescales, while partitioning of surfactant from water to oil, and oil solubilization into the water, act on longer timescales to facilitate the complete dewetting. Understanding of the

* Corresponding author.
E-mail addresses: kuk197@psu.edu (K.E. Kim), wzx5066@psu.edu (W. Xue), ldz4@psu.edu (L.D. Zarzar).
[1] Authors contributed equally to this work.
[2] Address: 104 Chemistry Building, University Park, PA 16802, USA.

https://doi.org/10.1016/j.jcis.2023.12.054
Received 17 September 2023; Received in revised form 2 December 2023; Accepted 8 December 2023
Available online 9 December 2023

role played by surfactant and oil transport presents opportunities for tailoring sessile droplet behaviors and controlling droplet dynamics under conditions that would previously not have been considered.

1. Introduction

Understanding the wetting properties of liquids on solid substrates is critical in a wide range of contexts including biomolecular condensates, [1,2] coatings, [3,4] cosmetics, [5] oil recovery, [6] ink-jet printing, [7] agricultural sprays, [8] and biochemical assays [9]. As such, the wettability and contact line dynamics of sessile droplets have been the focus of intense research interest for many decades, with the majority of prior studies focusing on evaporating water droplets in air [10–14]. However, sessile droplets that lack a liquid–air interface, such as an oil droplet wetted to a substrate under water, are also commonly encountered. Given that sessile oil droplets in water have a liquid–liquid interface across which molecules can partition, as well as an additional liquid–solid interface on which molecules can adsorb, such droplets may have different properties than those in air; these differences can potentially lead to non-intuitive wetting behaviors. For example, as we investigate herein, sessile oil droplets in aqueous surfactant can, in some cases, preferentially spread on hydrophilic planar substates but dewet from hydrophobic substrates.

The equilibrium contact angle (θ) of a sessile droplet is described for ideal surfaces by Young's equation,

$$\gamma_S = \gamma_{SL} + \gamma_L \cos\theta \tag{1}$$

where, γ_S, γ_{SL}, and γ_L represent the solid surface energy, solid–liquid interfacial tension, and liquid surface tension respectively. As captured by **Eq. (1)**, changes in interfacial tensions will be reflected in the contact angle of the droplet. Accordingly, the inclusion of a surface-active chemical inside the droplet or surrounding environment can modify the wetting behavior of the droplet. For example, sessile water drops containing the surfactant cetyltrimethylammonium bromide (CTAB) wetted to glass in air undergo adsorption-induced dewetting due to modification of the solid–liquid interfacial tension, [15] and the contact angle of a water—1,2-hexanediol droplet in air has been observed to be unexpectedly high due to Marangoni contraction and autophobing [16]. Introduction of a liquid environment surrounding the sessile droplet adds more opportunities for complex mass transfer effects, especially when a chemical species can partition across the liquid–liquid interface. For example, sessile pentanol-cyclohexane droplets in water exhibit a non-homogeneous spatial distribution of chemical components within the droplet due to differences in solubility between the pentanol and cyclohexane in water, resulting in Marangoni flows and superspreading [17].

In this paper, we explore the wetting properties of sessile, solubilizing oil droplets in aqueous surfactant solution, considering the case in which surfactant can transfer from the water into the droplet [18–20]. This study was motivated by an observation of sessile 1-bromohexane oil droplets in aqueous Tergitol NP-9 nonionic surfactant solution undergoing complete dewetting from a hydrophobized substrate while spreading on a hydrophilic substrate. Although this counterintuitive dynamic behavior bears similarity to the autophobing effect, the time scales that we observe for the dewetting/spreading process (tens of minutes) is considerably longer than is typical for autophobing systems (timescale of seconds) [15,21]. Using optical microscopy to investigate the contact line dynamics and droplet profile, we analyze the dependence of the dewetting on droplet size and surfactant concentration. We find that the non-intuitive wetting behavior of 1-bromohexane is the result of both surfactant adsorption and partitioning effects which work synergistically on different timescales; effects of adsorption are quickly evidenced but the effects of surfactant partitioning unfold over longer times. By using an oil such as 1-bromohexadecane that does not significantly partition surfactant, we deconvolute the relative importance of surfactant adsorption and partitioning in governing wetting behavior. The same adsorption and partitioning-driven mechanisms explain the spreading of 1-bromohexane and 1-bromohexadecane on a hydrophilic substrate. We further examine the dewetting behaviors of bromoalkanes in different surfactants including Tergitol NP-15 and sodium dodecylsulfate (SDS). The importance of liquid–liquid surfactant partitioning in the counter-intuitive wetting behavior exemplifies how sessile droplets in aqueous environments are subject to transport processes not encountered in air. The transport of surfactant provides an opportunity to engineer sessile droplet behaviors over varying timescales and introduces new considerations for how to formulate surfactants and fabricate substrates for desired wetting dynamics in contexts such as cosmetics and oil recovery.

2. Materials and methods

For a more detailed experimental methods, refer to the Supporting Information.

2.1. Chemicals

1-bromohexane (>98 %) (Alfa Aesar); 1-bromohexadecane (>98 %) (Alfa Aesar); 1-iodohexadecane (>98 %) (Alfa Aesar); (Alfa Aesar); hexanes (98.5 %) (Fischer Scientific); Tergitol NP-9 (Sigma) (see **Fig. S1** for mass spectrometry graph showing surfactant purity); Tergitol NP-15 (Dow); sodium dodecylsulfate (>99.0 %) (Sigma-Aldrich); hexadecyltrimethoxysilane (95 %) (Ambeed); silicon wafers (Prime grade, P/Boron dopant, 525 ± 25 μm thickness); reagent alcohol (94–96 %) (VWR); toluene (99.5 %) (Honeywell); sulfuric acid (95–98 %)(GR ACS); hydrogen peroxide (30 %) (Ward's science).

2.2. Piranha cleaning of silicon wafers

Silicon wafers were triple washed with DI water and immersed in piranha solution (3:1 vol ratio of sulfuric acid and hydrogen peroxide). The piranha-cleaned wafers were stored in a petri dish filled with deionized water to prevent contamination.

2.3. Hydrophobic surface functionalization of silicon wafers

Piranha-cleaned silicon wafers were allowed to react overnight in a solution of 100 mL of 1.0 v.% hexadecyltrimethoxysilane in hexanes and 200 μL of diethylamine. Silicon wafers were placed into the silane solution with the polished side of the wafer exposed to the bulk solution and left to react overnight. Wafers were rinsed with hexanes and ethanol and then stored in air.

2.4. Verification of surface functionalization via water contact angle measurement

To check the consistency of the surface functionalization, water contact angle measurements on the treated silicon wafers were conducted immediately before use. Three water contact angle measurements were collected with a Ramé-hart 250-U1-R automatic goniometer. Substrates were only used if the average contact angle over three trials was near 105° for the hydrophobic substrate and 30° for the hydrophilic substrate.

2.5. Description of imaging setup for observation of droplet dynamics over time

To image the wetted droplet from the side, an in-house transmission microscope composed of a white LED for illumination, a microscope objective (10x, Nikon), and a 200 mm tube lens (Thorlabs) coupled to a CMOS camera (Basler) were used. The light and objective lens were oriented parallel to the substrate such that the side-view profile of the droplet could be recorded as a video over the course of the experiment.

2.6. Deposition of single oil droplets onto substrates

A microscope with the light source and objective lens oriented parallel to the sample substrate was used to allow visualization of the droplet profile as it wetted on the substrate in a glass cuvette (1 x 1 x 4 cm, L x W x H). Both the glass cuvette and substrate of choice were triple rinsed with methanol and DI water prior to use. Furthermore, all surfactant solutions were passed through a 0.45 μm nylon syringe filter before use. To create a single sessile microdroplet, a polydisperse oil-in-water emulsion was prepared by adding 10 μL oil to 0.025 wt% surfactant solution and shaking to emulsify; the specific surfactant used for emulsification and the subsequent dewetting/spreading experiment was kept constant. The emulsion was transferred to a glass dish and viewed using a transmission optical microscope (Nikon ECLIPSE Ts2 inverted microscope with 23UX249 color camera). A droplet of desired diameter was then selected using a micropipette and transferred to the cuvette with the desired substrate submerged in 0.5 mL DI water. The droplet was allowed to wet to the substrate, which typically took around a minute depending on the droplet composition. After the droplet wetted to the substrate and reached a stable contact angle, 0.5 mL of surfactant solution was added to produce the desired final surfactant concentration. Surfactant addition was visually observable due to the differing refractive indices between pure water and Tergitol NP-9. Solutions appeared homogeneous and clear approximately 100 s after surfactant addition, indicating that the surfactant is evenly distributed throughout solution. The recording was started (t = 0 s) at the moment of surfactant addition.

2.7. Image analysis for contact angle determination

Contact angles of the droplets observed by the side-view microscope were analyzed using the DropSnake plugin in ImageJ [22]. For all droplets, 8 points were manually selected along contour line of the droplet and the droplet profile was fit using spline-based image energy minimization to find the left and right contact angles. For every frame of interest, three contact angle measurements on both the left and right contact angles were collected and the average of all six contact angles were used as the mean contact angle. We define droplets which are motile (due to Marangoni flow) [23] to have contact angles of 180°; motile droplets exhibit smooth motion (Video S1) without any stick–slip behavior associated with the three-phase contact line, making it likely these droplets are not wetted to the substrate. To determine the steady-state contact angle, three contact angles spaced 5 min apart were collected and the associated standard deviation was calculated. If the standard deviation is smaller than 3°, then the average of the three points is considered as the steady-state contact angle.

3. Results and discussion

3.1. Observation of 1-bromohexane oil dewetting and spreading behaviors

We first noticed the aforementioned counterintuitive dewetting behavior when observing a sessile 1-bromohexane micro-droplet on a hexadecyltrimethoxysilane-functionalized silicon wafer ("hydrophobic substrate," water contact angle of 105.8° ± 3.1°) in aqueous 1 wt% Tergitol NP-9. Tergitol NP-9 is a common nonionic nonylphenol ethoxylate surfactant with an average of 9 ethylene oxide repeat units in the headgroup (**Fig. S1**). To create the sessile droplet, we emulsified 1-bromohexane in 0.025 wt% Tergitol NP-9 and transferred a single 200 μm diameter droplet into a cuvette containing the hydrophobic substrate in deionized water. The dense oil droplet sank and wetted to the substate, yielding a stable contact angle. Aqueous Tergitol NP-9 surfactant solution was then added to the cuvette to yield a final concentration of 1 wt% (Fig. 1a). As this surfactant concentration is well above the critical micelle concentration (CMC) of 0.006 wt%, the oil from the droplet solubilized into micelles, causing the droplet volume to decrease over time. However, rather than exhibiting contact angle stick–slip behavior as is typically expected in sessile droplets of shrinking volume, [24,25] the oil droplet dewetted from the hydrophobic substrate to a contact angle of 180° over a period of minutes (Fig. 1b, top row; **Video S1**). We also observed the same dewetting behavior on the hydrophobic substrate for oils less dense than water, such as toluene (**Fig. S2**). When the same experiment was repeated with a hydrophilic native silicon oxide substrate ("hydrophilic substrate", water contact angle of 29.4° ± 0.8°), the droplet initially wetted with a higher contact angle than on the hydrophobic substrate and then spread such that the final contact angle was substantially lower (Fig. 1b, bottom row; **Video S2**).

The complete dewetting of the oil droplet on the hydrophobic substrate and spreading on the hydrophilic substrate was surprising to us. Typically, hydrophobic liquids preferably spread on hydrophobic surfaces. This expectation comes from the fact that hydrophobic oils tend to have a low solid-oil interfacial tension (γ_{SO}) on hydrophobic surfaces, resulting in a low contact angle (θ) according to Young's equation (**Eq. (1)**). Conversely, oils typically have a higher γ_{SO} on hydrophilic substrates, resulting in a higher θ. Indeed, we found that 1-bromohexane has a lower γ_{SO} on the hydrophobic substrate compared to the hydrophilic substrate (0.9 ± 0.5 mN/m versus 41.7 ± 1.4 mN/m, **Tables S1-S2**). Furthermore, the timescale for both dewetting and spreading (~14 min) was considerably longer than expected for autophobing droplets [15,26], making the observed behavior even more puzzling.

3.2. Surfactant adsorption and dewetting

We considered what might be leading to the unexpected wetting behaviors. For simplicity, we focused first on the case of dewetting from the hydrophobic substrate for our analysis. Unlike evaporating or dissolving sessile droplets in a surfactant-free environment, a clear difference in our system is the presence of a surfactant that can adsorb to both the solid-water and oil-water interfaces, affecting both γ_{SW} and γ_{OW}. Because Tergitol NP-9 is an effective oil-in-water emulsifier, it was already known that γ_{OW} is greatly reduced in the presence of surfactant. We measured γ_{SW} for deionized water and aqueous 1 wt% Tergitol NP-9 on the hydrophobic substrate in air, also finding that γ_{SW} decreased from 42.1 ± 3.8 mN/m to 1.9 ± 1.1 mN/m with the introduction of the surfactant (**Table S1**). To consider the impact of surfactant adsorption on the contact angle, we rearrange Young's equation (**Eq. (1)**) as:

$$\frac{\gamma_{SW} - \gamma_{SO}}{\gamma_{OW}} = \cos\theta \tag{2}$$

As gleaned from **Eq. (2)**, a decrease in γ_{SW} always corresponds to an increase in θ assuming a constant value of γ_{SO} (0.9 ± 0.5 mN/m for pure 1-bromohexane on the hydrophobic substrate). However, the effect of decreasing γ_{OW} on θ is uncertain because it depends on whether γ_{SW}–γ_{SO} is positive or negative. If the dewetting behavior was governed by surfactant adsorption onto the solid-water interface and lowered γ_{SW}, then we would expect that the dewetting kinetics should be largely independent of droplet size. To test this, we conducted the same dewetting experiment on the hydrophobic substrate with a larger 300 μm diameter 1-bromohexane droplet in 1 wt% Tergitol NP-9. (The diameter corresponds to the droplet prior to wetting, refer to Fig. 1a). We found that the larger 300 μm droplet took significantly longer to dewet to $\theta = 180°$ (28 ± 7 min, average and standard deviation from 3 trials) than the 200

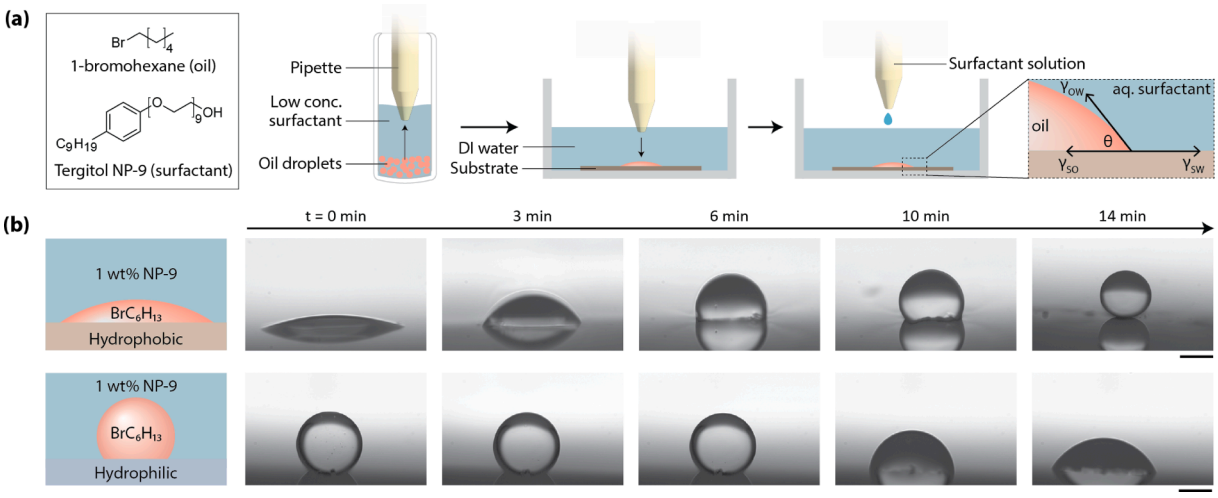

Fig. 1. 1-Bromohexane in aqueous surfactant displays unexpected dewetting and spreading behaviors on hydrophobic and hydrophilic substrates, respectively. a) Chemical structures of the 1-bromohexane oil and Tergitol NP-9 surfactant ("NP-9") along with the general experimental procedure used to produce a sessile microdroplet in this work. Tergitol NP-9 is a polydisperse surfactant with an average of 9 ethylene oxide repeat units in the headgroup. Briefly, a polydisperse emulsion of 1-bromohexane droplets in low surfactant concentration (0.025 wt% Tergitol NP-9) was prepared. Within a few minutes of emulsification, a single droplet of desired volume was extracted by pipet and introduced to a glass cuvette containing water and substrate, which was either a hydrophobic silicon wafer (water contact angle of 105.8° ± 3.1°) or a hydrophilic silicon wafer (water contact angle of 29.4° ± 0.8°). The droplet settled to the substrate and wetted. After the droplet reached a stable contact angle, surfactant solution was then gently added to the cuvette to yield a final concentration of 1 wt%. **b)** A 200 μm diameter 1-bromohexane droplet dewetted to θ = 180° from the hydrophobic substrate (top, **Video S1**) and spread on the hydrophilic substrate (bottom, **Video S2**) in 1 wt% Tergitol NP-9 over the course of 14 min. t = 0 min was defined as the time of surfactant addition. Scale bars are 100 μm.

μm diameter droplet (13 ± 3 min, average and standard deviation from 6 trials; **Table S3**) (Fig. 2a). This droplet size dependence of the dewetting kinetics suggested that surfactant adsorption to the solid surface and reduction in γ_{SW} was likely not the only driver of dewetting from the hydrophobic substrate.

Considering that the smaller diameter droplet dewetted faster than the larger droplet, and smaller droplets have higher surface-area-to-volume ratios, we suspected that an additional contributing mechanism to the dewetting may be associated with partitioning across the oil-water interface. At the oil-water interface, the oil is not only transferred outwards into the water via solubilization, but the surfactant Tergitol NP-9—which is miscible with both the water and oil—also transfers into the oil droplet over time [18,19,27]. Previously, our group has found that the rate of non-equilibrium surfactant partitioning into oil droplets depends on droplet radius, with small droplets partitioning surfactant faster than large ones due to a larger surface area to volume ratio [20]. As such, we propose that the size-dependent dewetting of 1-bromohexane stems from the size-dependent rate of surfactant partitioning. Analyzing the impact of partitioning on wetting behavior, we found that higher concentrations of the surfactant inside the 1-bromohexane oil cause an increase in γ_{SO}, presumably since Tergitol NP-9 carries polar ethoxylate headgroups that interact unfavorably with the hydrophobic substrate (**Fig. S3**). As reflected in **Eq. (2)**, an increase in γ_{SO} corresponds to a larger θ, indicating that surfactant partitioning into 1-bromohexane may work in tandem with the surfactant adsorption to produce an increase in θ.

3.3. *Ultra-low γ_{OW} from surfactant partitioning contributes to dewetting*

Knowing that a surfactant adsorption-driven decrease in γ_{SW} and a partitioning-driven increase in γ_{SO} both contribute to dewetting of the 1-bromohexane, the last variable left to consider was γ_{OW}. When observing the fully dewetted (θ = 180°) 1-bromohexane droplet in 1 wt% Tergitol NP-9 over the timescale of hours, we noticed that the droplet

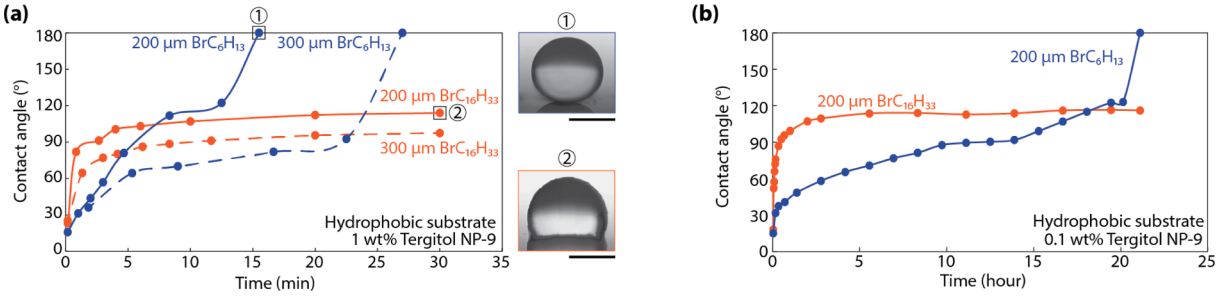

Fig. 2. Dewetting of 1-bromoalkanes in Tergitol NP-9 on hydrophobic substrates depends on oil alkyl chain length and droplet size. a) The droplet contact angle as a function of time for sessile droplets of 1-bromohexane (blue) and 1-bromohexadecane (orange) with initial drop spherical diameters of 200 μm (solid line) and 300 μm (dashed line) in 1 wt% Tergitol NP-9 on a hydrophobic substrate. The smaller bromohexane droplets dewetted faster than the larger ones, reaching θ = 180° within 13 ± 3 min, whereas the larger droplets took 28 ± 7 min. The 1-bromohexadecane droplets did not demonstrate significant size dependence both droplet sizes approached the steady-state contact angle within the first few minutes. **b)** Contact angle as a function of time for 200 μm diameter 1-bromohexane (blue) and 1-bromohexadecane (orange) droplets on a hydrophobic substrate in 0.1 wt% Tergitol NP-9. Both oils demonstrate a sharp increase in θ at early times which we attribute to surfactant surface adsorption, but the 1-bromohexane takes approximately 21 h to fully dewet, which we attribute to the effects of surfactant partitioning. Note that all curves show data from a single representative droplet. (For interpretation of the references to color in this figure legend, the reader is referred to the web version of this article.)

transformed from spherical to a more flattened ellipsoid, deforming considerably under gravity (Fig. S4). This deformation implies that the oil-water interfacial tension became very low, since body-forces typically do not dominate at small length scales. When we attempted to quantify γ_{OW} for 1-bromohexane in 1 wt% Tergitol NP-9 using pendant drop tensiometry, the droplet always fell off the dispensing needle before the steady-state γ_{OW} was reached, preventing an accurate measurement (Fig. S5). Instead, we used a microdroplet deformation-based geometric analysis (see **Supporting Information** section "Estimation of γ_{OW} for 1-bromohexane in Tergitol NP-9") to conservatively estimate a steady-state γ_{OW} on the order of 10^{-3} mN/m for 1-bromohexane in 1 wt% Tergitol NP-9. This is five orders of magnitude lower than γ_{OW} of 1-bromohexane in deionized water (37.57 ± 1.00 mN/m) and two orders of magnitude lower than γ_{OW} of 1-bromohexadecane 1 wt% Tergitol NP-9 (0.44 ± 0.03 mN/m) (Table S4).

We consider the mechanism governing this ultra-low oil-water interfacial tension. The surfactant Tergitol NP-9 is miscible in both the bromohexane and the water, and thus it can partition into the oil droplet; we previously studied partitioning of Tergitol NP-9 into bromooctane and found that even at concentrations of 0.1 w/v% Tergitol NP-9 in the water, concentrations of the surfactant in the oil droplet reached over 7 w/v% [20]. Given that bromooctane is more hydrophobic than bromohexane, and we are using higher aqueous concentrations of Tergitol NP-9, it is reasonable to expect that the concentration of surfactant inside the droplet is higher than 7 w/v%. Even after the bromohexane droplet reaches a steady state surfactant concentration, it continues to solubilize and shrink in volume, releasing both oil and surfactant into the vicinity of the oil-water interface [20]. As the composition of the aqueous phase near the droplet becomes more chemically similar to the droplet itself, we believe that this causes a significant interfacial tension decline. We have also previously observed this phenomenon in other oil droplets that partition surfactant [20]. The continuous decline in γ_{OW} happens over the hours long timescale for micro-droplets, far slower than the timescale for surfactant adsorption [28,29].The ultra-low γ_{OW} for 1-bromohexane relates to the contact angle of the droplet as dictated by **Eq. (1)**. In Young's equation (**Eq. (1)**), a decrease in γ_{OW} combined with a negative γ_{SW}–γ_{SO} corresponds to an increase in contact angle. Since γ_{SW} is 1.9 ± 1.1 mN/m for aqueous 1 wt % Tergitol NP-9 and γ_{SO} is 2.8 ± 0.1 mN/m for 1-bromohexane containing 10 wt% Tergitol NP-9 (Fig. S3), it is reasonable that the partitioning-driven decrease in γ_{OW} aids in dewetting the droplet at longer times. Moreover, the low γ_{OW} may amplify the effects of line tension on the contact angle, which are often ignored when analyzing sessile droplets on the macroscale and microscale [30]. The apparent line tension τ, defined as the excess free energy per unit length of the three-phase contact line, can impact θ according to the modified Young's equation,

$$\cos\theta = \cos\theta_0 - \frac{\tau}{\alpha\gamma_L} = \cos\theta_0 - \bar{\tau} \quad (3)$$

where $\bar{\tau}$ is a dimensionless correction factor that accounts for line tension, α is the radius of the solid–liquid contact area, and θ_0 is the contact angle of the droplet neglecting line tension. As the correction factor for line tension $\bar{\tau}$ in **Eq. (3)** increases with decreasing γ_{OW}, the ultra-low γ_{OW} caused by surfactant partitioning may cause line tension to be a significant driving force for dewetting. Given that the apparent line tension is largely caused by body forces on the droplet, [31] it is possible that an ultra-low γ_{OW} would allow gravitational forces to dominate and thus significantly impact the contact angle. Contributions from line tension may also help to explain the abrupt jump in θ occurring at around 120° to 180° that is consistently observed for 1-bromohexane; this may be due to $\bar{\tau}$ reaching a critical value at which the sessile droplet undergoes a wetting transition [32]. Thus, we propose that γ_{OW} reduces to ultra-low values for 1-bromohexane as a consequence of surfactant partitioning and solubilization, acting as an additional driving force for dewetting. This solubilization/partitioning-driven decrease in γ_{OW} occurs well past the timescale for surfactant adsorption, explaining why the dewetting of 1-bromohexane takes much longer compared to previously studied dewetting of sessile droplets in air which are controlled by adsorption [15,16].

3.4. Deconvoluting the effects of surfactant surface adsorption and liquid phase partitioning

To investigate the relative importance of surfactant partitioning and surface adsorption to the dewetting, we tested the dewetting of a more hydrophobic oil, 1-bromohexadecane, which due to the higher carbon number does not partition as much surfactant as the bromohexane [20,33] and does not solubilize to a measurable extent [23]. Because pure 1-bromohexadecane is less dense than water, which is experimentally inconvenient, we added 10 wt% of 1-iodohexadecane to increase the density to 1.0091 g/mL. In 1 wt% Tergitol NP-9, the 200 μm and 300 μm diameter 1-bromohexadecane droplets dewetted on the hydrophobic substrate from 19 ± 4° and 25 ± 3° to steady-state contact angles of 99 ± 4° and 87 ± 11° within 3 min respectively (Fig. 2a). Thus, the dewetting of 1-bromohexadecane droplet exhibited no significant dependence on droplet size, unlike 1-bromohexane. Moreover, the timescale for reaching the steady state contact angle was significantly faster for 1-bromohexadecane than the 1-bromohexane (approximately 3 min vs 15 min for the 200 μm diameter drops) (Fig. 2a), which aligns with the expectation that surfactant adsorption occurs on a shorter timescale than partitioning and indicates that the dewetting of 1-bromohexadecane is primarily adsorption-driven [34].

As surfactant adsorption, partitioning, and solubilization are distinct molecular processes with many proposed kinetic models, [35,36] we were curious how lowering the aqueous surfactant concentration would impact dewetting kinetics. We examined the dewetting of 200 μm-diameter droplets of 1-bromohexane and 1-bromohexadecane on the hydrophobic substrate in an order-of-magnitude lower surfactant concentration, 0.1 wt% Tergitol NP-9 (Fig. 2b). Both oils established similar steady-state contact angles in 1 wt% and 0.1 wt% Tergitol NP-9, however the time needed to reach steady-state at 0.1 wt% was two orders-of-magnitude longer than 1 wt% likely due to slower adsorption and partitioning kinetics. At any given surfactant concentration, both droplets are affected by the same adsorption process at the solid-water interface. However, the behaviors of the two droplets clearly diverge after the first few hours, with 1-bromohexadecane establishing a steady-state contact angle of 110 ± 7° and the 1-bromohexane continuing to dewet to a final contact angle of 180° over 15 h later. As most of the contact angle change for 1-bromohexane occurs after the timescale for adsorption-driven dewetting, we reason that the dewetting of 1-bromohexane is primarily partitioning-driven.

3.5. Consideration of spreading behavior on the hydrophilic substrate

Until now, we have investigated dewetting of oil droplets on the hydrophobic substrate; however, the hydrophilic substrate presents different solid-water and solid-oil interfaces compared to the hydrophobic substrate, consequently modifying the impact of surfactant adsorption and partitioning. Both 200 μm-diameter 1-bromohexane and 1-bromohexadecane droplets spread on the hydrophilic substrate rather than dewet (Fig. 3a), indicating that the surfactant induces different changes in γ_{SW} and γ_{SO} compared to the case of dewetting on the hydrophobic substrate. For the hydrophilic substrate, addition of Tergitol NP-9 causes an increase in γ_{SW} from 3.9 ± 0.5 mN/m in water to 36.1 ± 0.3 mN/m in 1 wt% Tergitol NP-9 (Fig. 3b) likely due to unfavorable interactions between the hydrophobic tail of the surfactant and hydrophilic substrate, while partitioning of Tergitol NP-9 into the 1-bromohexane droplet decreases γ_{OW} and γ_{SO} (Fig. S6). The increase in γ_{SW} and decrease in γ_{SO} and γ_{OW} corresponds to a decrease in contact angle as per **Eq. (1)** and **Eq. (3)**, explaining the observed spreading on the

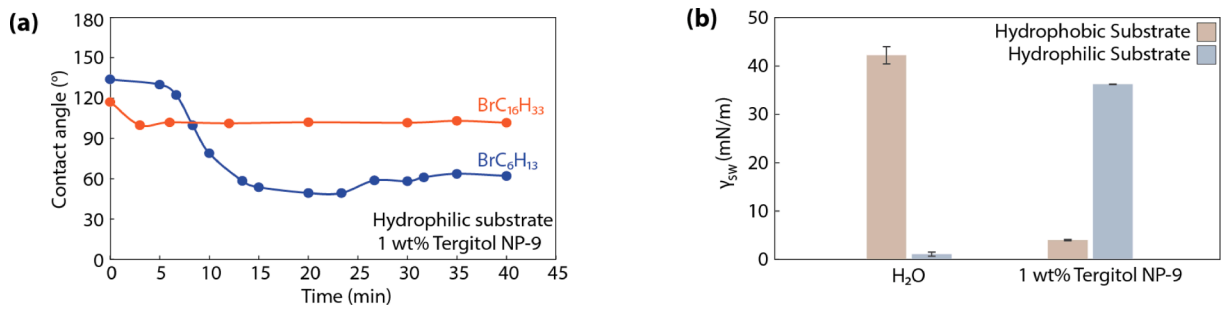

Fig. 3. Spreading of 1-bromoalkane droplets on the hydrophilic substrate in 1 wt% Tergitol NP-9. a) Contact angle (°) vs time (min) for 200 μm diameter 1-bromohexane (blue) and 1-bromohexadecane (orange) droplets in 1 wt% Tergitol NP-9 on the hydrophilic substrate. Diameter corresponds to the spherical droplet prior to wetting to the substrate. Each curve is data for one representative droplet. **b)** Solid-water interfacial tension on the hydrophobic and hydrophilic substrates before and after addition of Tergitol NP-9 to the aqueous phase. Surfactant addition causes γ_{SW} to decrease on the hydrophobic substrate and increase on the hydrophilic substrate, reflecting the dewetting and spreading behaviors on each substrate respectively. (For interpretation of the references to color in this figure legend, the reader is referred to the web version of this article.)

hydrophilic substrate. In contrast, we recall that on the hydrophobic substrate, surfactant adsorption decreases γ_{SW} from 42.1 ± 3.8 mN/m in deionized water to 1.9 ± 1.1 mN/m in 1 wt% Tergitol NP-9 (Fig. 3b), while surfactant partitioning decreases γ_{OW} and increases γ_{SO} (**Fig. S3**). The different directions of change in γ_{SW} and γ_{SO} (i.e., increase vs decrease) for the hydrophilic and hydrophobic substrates ultimately causes droplets to have divergent behaviors (spreading vs dewetting).

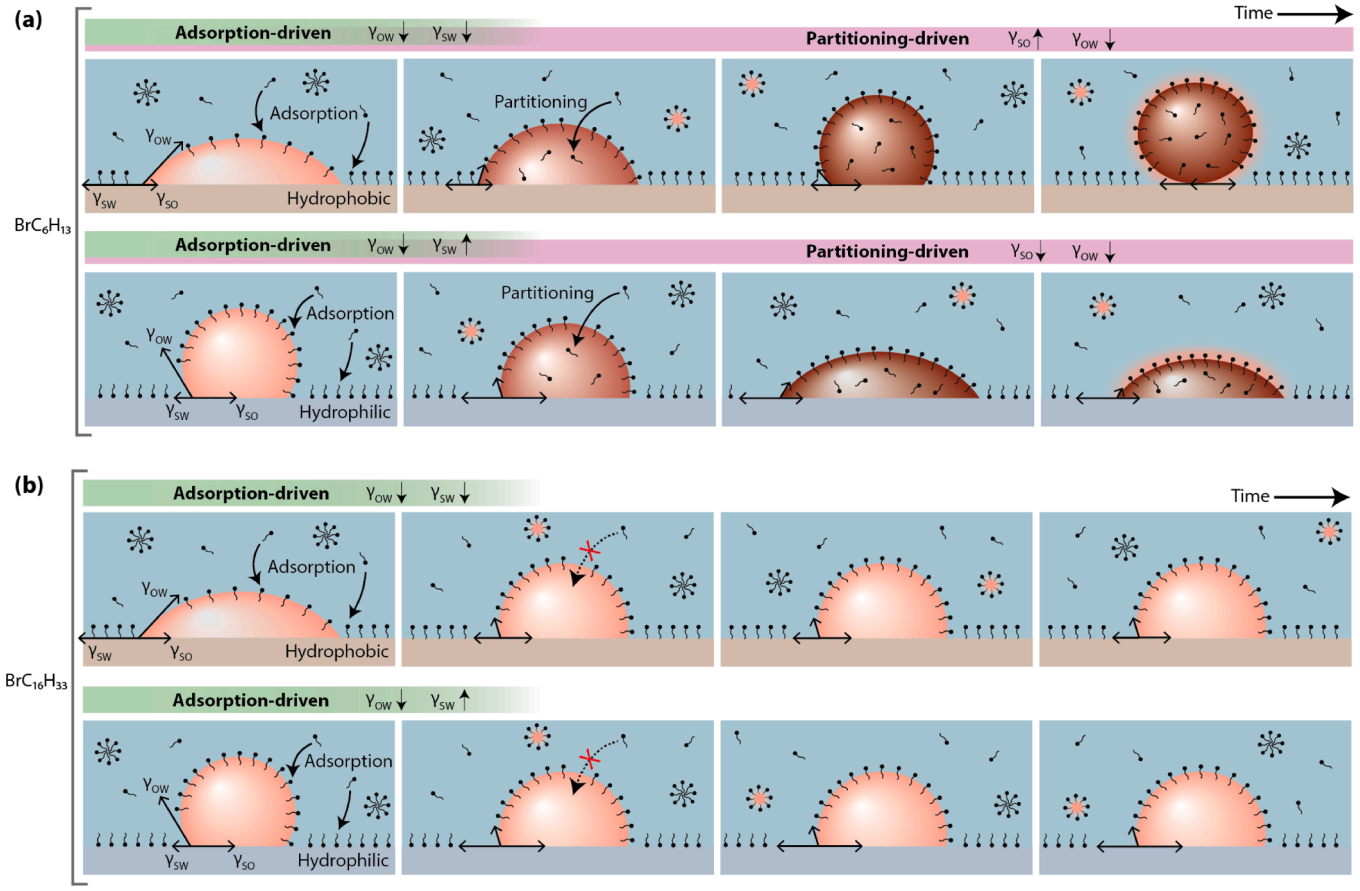

Fig. 4. Schematic of proposed dewetting and spreading mechanism. a) For 1-bromohexane, surfactant adsorption causes dewetting (spreading) on hydrophobic (hydrophilic) substrates at shorter timescales as surfactant saturates the solid-water and oil-water interfaces. Over a longer timescale relative to surface adsorption, surfactant partitioning into the droplet modifies the solid-oil interfacial tension (γ_{SO}). Partitioning in combination with solubilization leads to a further reduction in oil-water interfacial tension, γ_{OW}, also over longer timescales. b) For 1-bromohexadecane, an oil which does not significantly partition surfactant nor solubilize, surfactant adsorption to the solid-water and oil-water interfaces governs the contact angle dynamics. The contact angle thus reaches steady state far faster than the 1-bromohexane. Note that on the hydrophilic substrate, surfactant may not necessarily be adsorbed in a monolayer as depicted here.[37] Although adsorption and partitioning are depicted as involving single surfactant molecules here, both processes may (and are likely to) involve different chemical species (e.g. micelles) at the molecular level. The drawings are not to scale, and the magnitudes of the interfacial tension vectors are drawn schematically to show the trends but are not to scale with the measured values reported in **Tables S1-S2** and **Tables S4**.

3.6. Summary of mechanism for dewetting and spreading droplets

We find that the dewetting of bromoalkanes on the hydrophobic substrate and spreading on the hydrophilic substrate is the result of both surfactant adsorption-driven and partitioning-driven processes, which are visually summarized in Fig. 4. On shorter timescales, surfactant adsorption to the solid-water and oil-water interface results in initial dewetting (or spreading, substrate dependent). Oils that have negligible surfactant partitioning (e.g. 1-bromohexadecane, Fig. 4b) reach the steady-state contact angle after the interfaces are saturated with surfactant. However, oils which partition a significant amount of surfactant (e.g. 1-bromohexane, Fig. 4a) as well as solubilize, undergo further changes in γ_{SO} and γ_{OW} over longer timescales. Essentially, adsorption and partitioning modify the Gibbs free energy of the solid-water, solid-oil, and oil-water interfaces, causing the system to reconfigure (via change in contact angle) to reduce overall system free energy. The role of partitioning in modifying the solid-oil and oil-water interfaces causes 1-bromohexane to display significant changes in the contact angle at timepoints well beyond those typically considered for contact angle dynamics of sessile droplets in air, and the timescale for dewetting/spreading is determined by the kinetics of adsorption, partitioning, and solubilization which can be affected by factors such as surfactant concentration.

3.7. Influence of different surfactants on dewetting

As the surfactant molecular structure (Tergitol NP-9) was kept constant through all prior experiments, we were curious how different surfactants impact the behavior of sessile oil-in-water droplets on the hydrophobic substrate. We first tested the dewetting of 1-bromohexane and 1-bromohexadecane in Tergitol NP-15, which has an average of 15 ethylene oxide repeats units in the headgroup (which is six more units than in the hydrophilic head group of Tergitol NP-9) and consequently has a higher hydrophilic-lipophilic balance (HLB) value of 15.0 vs 12.9 for Tergitol NP-9. We found that neither 1-bromohexane nor 1-bromohexadecane dewetted in 1 wt% Tergitol NP-15 on the hydrophobic substrate (Fig. 5a). The lack of change in contact angle is likely due to the fact that Tergitol NP-15 does not reduce γ_{SW} as significantly as Tergitol NP-9 ($\gamma_{SW} = 42.1 \pm 3.8$ mN/m in DI water; $\gamma_{SW} = 9.81 \pm 1.02$ mN/m for 1 wt% Tergitol NP-15 vs 1.89 ± 1.1 mN/m for 1 wt% Tergitol NP-9), corresponding to a smaller increase in θ (**Eq. (1)**). Furthermore, we expect partitioning of Tergitol NP-15 into the oil to be much reduced due to the surfactant's increased hydrophilicity (higher HLB), resulting in weak partitioning-driven dewetting that may not be reflected in the apparent contact angle due to contact line pinning. We note that the relation between a surfactant's CMC and the dewetting behavior is non-obvious and requires further investigation (see "Relation between the CMC and dewetting" in the SI).

A second surfactant system in which we were interested was mixed nonionic surfactant (Tergitol NP-9) and anionic surfactant (sodium dodecylsulfate, SDS) due to the prevalence of mixed surfactant use in industrial settings [38]. As a control, we first tested the dewetting of 200 μm diameter 1-bromohexane and 1-bromohexadecane droplets in 1 wt% SDS on the hydrophobic substrate (Fig. 5b–c), finding that neither droplet changes contact angle over time. This result likely has similar reasoning to the case of Tergitol NP-15, where γ_{SW} does not decrease as significantly as in Tergitol NP-9, with measured values of 10.4 ± 0.2 mN/m in 1 wt% SDS versus 1.89 ± 1.1 mN/m for 1 wt% Tergitol NP-9 ($\gamma_{SW} = 42.1 \pm 3.8$ mN/m in DI water). The relative inefficacy of SDS at reducing the solid-water interfacial tension is likely due to repulsive charge in the head group which causes SDS to pack at the interface less densely than the nonionic Tergitol NP-9. Partitioning is also negligible due to the low solubility of the SDS in the oil. Next, testing the same droplets in a mixture of 1 wt% Tergitol NP-9 and 0.1 wt% SDS, the 1-bromohexane showed no observable dewetting in the mixed surfactant (Fig. 5b) while the 1-bromohexadecane dewetted to a steady-state $\theta = 64° \pm 2°$ (Fig. 5c). For 1-bromohexane which is primarily affected by partitioning-driven dewetting, the inhibition of Tergitol NP-9 partitioning into the oil by SDS (which forms mixed micelles) [27] likely eliminates the main driving force for dewetting, resulting in negligible change of contact angle. For 1-bromohexadecane, the steady-state contact angle in the mixed surfactant solution ($66° \pm 1°$) between the steady-state contact angles for pure Tergitol NP-9 ($99° \pm 4°$) and SDS ($25° \pm 2°$) is likely due to the formation of a mixed surfactant monolayer at the solid-water interface, resulting in a γ_{SW} between the values for 1 wt% Tergitol NP-9 and 1 wt% SDS and suppressed adsorption-driven dewetting compared to pure 1 wt% Tergitol NP-9. As such, we suggest that the ionic nature of SDS suppresses partitioning-driven dewetting and correspondingly leads to less dewetting compared to the nonionic Tergitol NP-9. Broadly, changes in surfactant chemistry significantly impact droplet behavior, highlighting the complexity presented by the seemingly simple system of a sessile oil droplet in surfactant solution.

4. Conclusions

Sessile oil droplets in surfactant solution are commonly encountered, such as in oil drilling and recovery [6] or surface cleaning [3], but the dynamic contact angle characteristics of such droplets are not well understood. In particular, in situations where the surfactant and oil can each partition across the oil-water interface, non-equilibrium bi-directional transport plays a role and can lead to unexpected behaviors. Here, we have investigated how aqueous surfactant partitioning and surfactant-mediated oil solubilization impact sessile oil droplet contact line dynamics. We observed unusual and counterintuitive contact line behaviors compared to sessile droplets in air [39–41]: oil droplets dewetted from hydrophobic substrates but spread on hydrophilic

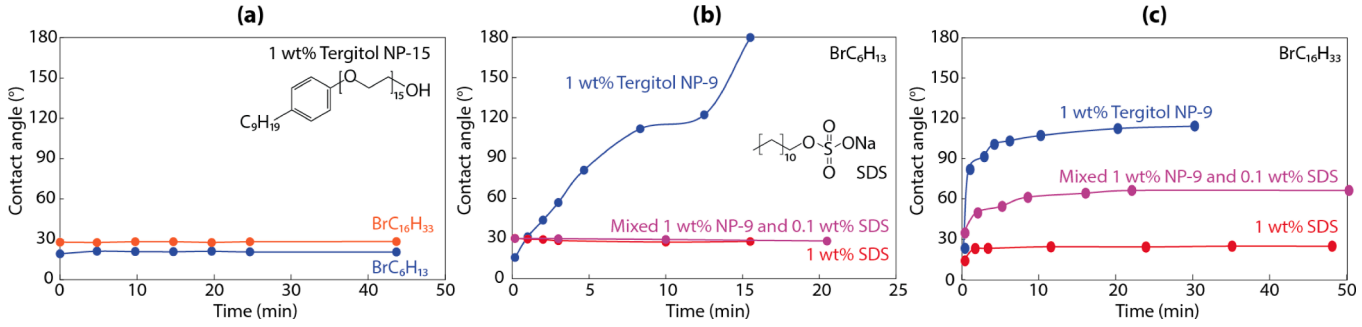

Fig. 5. Surfactant composition effects on wetting dynamics. a) Neither 1-bromohexane nor 1-bromohexadecane dewetted from the hydrophobic substrate in 1 wt % Tergitol NP-15. **b)** 1-Bromohexane did not dewet in 1 wt% SDS. Doping 1 wt% Tergitol NP-9 with 0.1 wt% SDS eliminates all dewetting of 1-bromohexane on the hydrophobic substrate. **c)** 1-Bromohexadecane dewetted to a lesser degree in 1 wt% SDS compared to 1 wt% Tergitol NP-9. Doping 1 wt% Tergitol NP-9 with 0.1 wt% SDS caused 1-bromohexadecane to dewet to an intermediate steady-state contact angle. All droplets were 200 μm in diameter prior to wetting. Each data point represents a single measurement.

substrates under conditions where surfactant partitioned into the oil. While evaporating sessile droplets in air typically exhibit fluctuations on the order of ~ 10-30° in contact angle around the equilibrium value due to contact angle hysteresis [42,43], we found that solubilizing sessile oil drops in aqueous surfactant may change their contact angle by up to ~ 160° over timescales that depend significantly on the surfactant concentration and droplet size; some droplets examined took over a day to reach a steady state contact angle. By examining the dewetting kinetics while varying droplet size, composition, and surfactant concentration, we conclude that the dewetting of oil from a hydrophobic substrate and spreading on a hydrophilic substrate arises from the combination of surfactant adsorption, surfactant partitioning, and oil solubilization processes. The bidirectional transfer of components (i.e. surfactant transferring into oil and oil transferring into water) is not typically necessary to consider for sessile drops in air [14,21]. The presence and significance of each mechanism in driving dewetting or spreading is dependent on the oil and surfactant molecular structure; oils like 1-bromohexane or toluene that have a greater propensity to uptake the polar surfactants from the aqueous phase are more likely to dewet completely from the hydrophobic substrates, while oils that do not uptake surfactant appreciably, such as 1-bromohexadecane, have contact angles that are more so controlled by surfactant adsorption. The results presented here exemplify how sessile droplets in aqueous surfactant environments can behave unexpectedly compared to droplets in air due to surfactant transport. The importance of liquid–liquid partitioning in controlling wetting behavior may introduce new design considerations for relevant applications such as enhanced oil recovery or coatings. Furthermore, the insights from this study may potentially be relevant to understanding the influence of biomolecular liquid–liquid partitioning on the wetting of non-equilibrium cellular condensates which play a role in intracellular motion and spatial organization [1,2].

Declaration of competing interest

The authors declare the following financial interests/personal relationships which may be considered as potential competing interests: [Lauren Zarzar reports financial support was provided by Charles E Kaufman Foundation. Lauren Zarzar reports financial support was provided by Camille and Henry Dreyfus Foundation Inc. Lauren Zarzar reports financial support was provided by US Army Research Office].

Data availability

Data will be made available on request.

Acknowledgements

This work was financially supported by the Army Research Office (W911NF-18-1-0414), The Camille and Henry Dreyfus Foundation (TC-22-023) and the Charles E. Kaufman Foundation (1031373-438639).

Appendix A. Supplementary data

Supplementary data to this article can be found online at https://doi.org/10.1016/j.jcis.2023.12.054.

References

[1] B. Gouveia, Y. Kim, J.W. Shaevitz, S. Petry, H.A. Stone, C.P. Brangwynne, Capillary forces generated by biomolecular condensates, Nature. 609 (7926) (2022) 255–264, https://doi.org/10.1038/s41586-022-05138-6.
[2] A. Mangiarotti, N. Chen, Z. Zhao, R. Lipowsky, R. Dimova, Wetting and complex remodeling of membranes by biomolecular condensates, Nature Communications. 14 (1) (2023) 2809, https://doi.org/10.1038/s41467-023-37955-2.
[3] V.A. Ganesh, H.K. Raut, A.S. Nair, S. Ramakrishna, A review on self-cleaning coatings, J. Mater. Chem. 21 (41) (2011) 16304–16322, https://doi.org/10.1039/C1JM12523K.
[4] X. Yao, Y. Hu, A. Grinthal, T.-S. Wong, L. Mahadevan, J. Aizenberg, Adaptive fluid-infused porous films with tunable transparency and wettability, Nat. Mater. 12 (6) (2013) 529–534, https://doi.org/10.1038/nmat3598.
[5] K. Staszak, D. Wieczorek, K. Michocka, Effect of sodium chloride on the surface and wetting properties of aqueous solutions of cocamidopropyl betaine, J. Surfactant Deterg. 18 (2015) 21–328, https://doi.org/10.1007/s11743-014-1644-8.
[6] A.O. Gbadamosi, R. Junin, M.A. Manan, A. Agi, A.S. Yusuff, An overview of chemical enhanced oil recovery: Recent advances and prospects, International Nano Letters 9 (2019) 171–202, https://doi.org/10.1007/s40089-019-0272-8.
[7] P. Calvert, Inkjet printing for materials and devices, Chemistry of Materials 13(10) (2001) 3299-3305.https://doi.org/10.1021/cm0101632.
[8] I. Makhnenko, E.R. Alonzi, S.A. Fredericks, C.M. Colby, C.S. Dutcher, A review of liquid sheet breakup: Perspectives from agricultural sprays, J. Aerosol Sci. 157 (2021) 105805, https://doi.org/10.1016/j.jaerosci.2021.105805.
[9] G. McHale, Surface free energy and microarray deposition technology, Analyst. 132 (3) (2007) 192–195, https://doi.org/10.1039/B617339J.
[10] D. Daniel, M. Vuckovac, M. Backholm, M. Latikka, R. Karyappa, X.Q. Koh, J.V. I. Timonen, N. Tomczak, R.H.A. Ras, Probing surface wetting across multiple force, length and time scales, Communications Phys. 6 (1) (2023), https://doi.org/10.1038/s42005-023-01268-z.
[11] G. Oh, W. Jeong, N. Jung, S.H. Kang, B.M. Weon, Evaporation and deposition of colloidal binary droplets, Physical Review Applied. 17 (2) (2022) 024010, https://doi.org/10.1103/PhysRevApplied.17.024010.
[12] L. Zhao, S. Seshadri, X. Liang, S.J. Bailey, M. Haggmark, M. Gordon, M. E. Helgeson, J. Read de Alaniz, P. Luzzatto-Fegiz, Y. Zhu, Depinning of multiphase fluid using light and photo-responsive surfactants, ACS Cent. Sci. 8 (2) (2022) 235–245, https://doi.org/10.1021/acscentsci.1c01127.
[13] J.G. Kim, H.J. Choi, K.C. Park, R.E. Cohen, G.H. McKinley, G. Barbastathis, Multifunctional inverted nanocone arrays for non-wetting, self-cleaning transparent surface with high mechanical robustness, Small. 10 (12) (2014) 2487–2494, https://doi.org/10.1002/smll.201303051.
[14] L. Yang, A.A. Pahlavan, H.A. Stone, C.D. Bain, Evaporation of alcohol droplets on surfaces in moist air, Proc. Natl. Acad. Sci. 120 (38) (2023), https://doi.org/10.1073/pnas.2302653120 e2302653120.
[15] Y. Takenaka, Y. Sumino, T. Ohzono, Dewetting of a droplet induced by the adsorption of surfactants on a glass substrate, Soft Matter. 10 (30) (2014) 5597–5602, https://doi.org/10.1039/C4SM00798K.
[16] M.A. Hack, W. Kwiecinski, O. Ramírez-Soto, T. Segers, S. Karpitschka, E.S. Kooij, J. H. Snoeijer, Wetting of two-component drops: Marangoni contraction versus autophobing, Langmuir 37 (12) (2021) 3605–3611, https://doi.org/10.1021/acs.langmuir.0c03571.
[17] E. Dietrich, M. Rump, P. Lv, E.S. Kooij, H.J.W. Zandvliet, D. Lohse, Segregation in dissolving binary-component sessile droplets, J. Fluid Mech. 812 (2017) 349–369, https://doi.org/10.1017/jfm.2016.802.
[18] F. Ravera, M. Ferrari, L. Liggieri, Adsorption and partitioning of surfactants in liquid–liquid systems, Adv. Colloid Interface Sci. 88 (1–2) (2000) 129–177, https://doi.org/10.1016/S0001-8686(00)00043-9.
[19] M.A. Cowell, T.C. Kibbey, J.B. Zimmerman, K.F. Hayes, Partitioning of ethoxylated nonionic surfactants in water/NAPL systems: Effects of surfactant and NAPL properties, Environ. Sci. Tech. 34 (8) (2000) 1583–1588, https://doi.org/10.1021/es9908826.
[20] R. Balaj, W. Xue, P. Bayati, S. Mallory, L. Zarzar, Dynamic partitioning of surfactants into non-equilibrium emulsion droplets, Preprint on ArXiv. (2023), https://doi.org/10.26434/chemrxiv-2023-0t2w2.
[21] X. Zhong, F. Duan, Dewetting transition induced by surfactants in sessile droplets at the early evaporation stage, Soft Matter. 12 (2) (2016) 508–513, https://doi.org/10.1039/C5SM01976A.
[22] A.F. Stalder G. Kulik D. Sage L. Barbieri P. Hoffmann A snake-based approach to accurate determination of both contact points and contact angles Colloids and Surfaces a: Physicochemical and Engineering Aspects 286(1–3) 2006 92 103 10.1016/j.colsurfa.2006.03.008.
[23] C.M. Wentworth, A.C. Castonguay, P.G. Moerman, C.H. Meredith, R.V. Balaj, S. I. Cheon, L.D. Zarzar, Chemically tuning attractive and repulsive interactions between solubilizing oil droplets, Angew. Chem. Int. Ed. 61 (32) (2022) e202204510, https://doi.org/10.1002/anie.202204510.
[24] F. Wang, H. Wu, Molecular origin of contact line stick-slip motion during droplet evaporation, Sci. Rep. 5 (1) (2015) 17521, https://doi.org/10.1038/srep17521.
[25] E. Dietrich, E.S. Kooij, X. Zhang, H.J. Zandvliet, D. Lohse, Stick-jump mode in surface droplet dissolution, Langmuir. 31 (16) (2015) 4696–4703, https://doi.org/10.1021/acs.langmuir.5b00653.
[26] B. Bera, M.H. Duits, M.C. Stuart, D. Van Den Ende, F. Mugele, Surfactant induced autophobing, Soft Matter. 12 (20) (2016) 4562–4571, https://doi.org/10.1039/C6SM00128A.
[27] A. Graciaa, J. Lachaise, M. Bourrel, I. Osborne-Lee, R.S. Schechter, W. Wade, Partitioning of nonionic and anionic surfactant mixtures between oil/microemulsion/water phases, SPE Res Eng. 22 (03) (1987) 305–314, https://doi.org/10.2118/13030-PA.
[28] F. Tiberg, Physical characterization of non-ionic surfactant layers adsorbed at hydrophilic and hydrophobic solid surfaces by time-resolved ellipsometry, J. Chem. Soc. Faraday Trans. 92 (4) (1996) 531–538, https://doi.org/10.1039/FT9969200531.
[29] J.R. Campanelli, X. Wang, Dynamic interfacial tension of surfactant mixtures at liquid–liquid interfaces, J. Colloid Interface Sci. 213 (2) (1999) 340–351, https://doi.org/10.1006/jcis.1999.6149.

[30] J. Zhang, P. Wang, M.K. Borg, J.M. Reese, D. Wen, A critical assessment of the line tension determined by the modified Young's equation, Phys. Fluids. 30 (8) (2018), https://doi.org/10.1063/1.5040574.
[31] B.H. Tan, H. An, C.-D. Ohl, Body forces drive the apparent line tension of sessile droplets, Phys. Rev. Lett. 130 (6) (2023) 064003, https://doi.org/10.1103/PhysRevLett.130.064003.
[32] B. Widom, Line tension and the shape of a sessile drop, The J. Physical Chem. 99 (9) (1995) 2803–2806, https://doi.org/10.1021/j100009a041.
[33] G. Catanoiu, E. Carey, S. Patil, S. Engelskirchen, C. Stubenrauch, Partition coefficients of nonionic surfactants in water/n-alkane systems, J. Colloid Interface Sci. 355 (1) (2011) 150–156, https://doi.org/10.1016/j.jcis.2010.12.002.
[34] B. Riechers, F. Maes, E. Akoury, B. Semin, P. Gruner, J.-C. Baret, Surfactant adsorption kinetics in microfluidics, Proc. Natl. Acad. Sci. 113 (41) (2016) 11465–11470, https://doi.org/10.1073/pnas.1604307113.
[35] H. Diamant, D. Andelman, Kinetics of surfactant adsorption at fluid– fluid interfaces, J. Phys. Chem. 100 (32) (1996) 13732–13742, https://doi.org/10.1021/jp960377k.
[36] H. Mohrbach, Kinetics of nonionic surfactant adsorption at a fluid-fluid interface from a micellar solution, J. Chem. Phys. 123 (12) (2005), https://doi.org/10.1063/1.2036968.
[37] F. Tiberg, B. Joensson, J.-a. Tang, B. Lindman, Ellipsometry studies of the self-assembly of nonionic surfactants at the silica-water interface: Equilibrium aspects, Langmuir. 10 (7) (1994) 2294–2300, https://doi.org/10.1021/la00019a045.
[38] P.M. Holland, D.N. Rubingh, Mixed surfactant systems, Mixed surfactant systems, Am. Chem. Soc. (1992) 2–30, https://doi.org/10.1021/bk-1992-0501.ch001.
[39] R.D. Deegan, O. Bakajin, T.F. Dupont, G. Huber, S.R. Nagel, T.A. Witten, Capillary flow as the cause of ring stains from dried liquid drops, Nature. 389 (6653) (1997) 827–829, https://doi.org/10.1038/39827.
[40] A.-M. Cazabat, G. Guena, Evaporation of macroscopic sessile droplets, Soft Matter. 6 (12) (2010) 2591–2612, https://doi.org/10.1039/B924477H.
[41] R.G. Larson, Transport and deposition patterns in drying sessile droplets, AIChE J. 60 (5) (2014) 1538–1571, https://doi.org/10.1002/aic.14338.
[42] D. Orejon, K. Sefiane, M.E. Shanahan, Stick–slip of evaporating droplets: Substrate hydrophobicity and nanoparticle concentration, Langmuir. 27 (21) (2011) 12834–12843, https://doi.org/10.1021/la2026736.
[43] L. Gao, T.J. McCarthy, Contact angle hysteresis explained, Langmuir. 22 (14) (2006) 6234–6237, https://doi.org/10.1021/la060254j.